



FULL LENGTH ARTICLE

Pioglitazone ameliorates neuronal damage after traumatic brain injury via the PPAR γ /NF- κ B/IL-6 signaling pathway

Yongbing Deng ^{a,b}, Xue Jiang ^c, Xiaoyan Deng ^c, Hong Chen ^a, Jie Xu ^c, Zhaosi Zhang ^a, Geli Liu ^c, Zhu Yong ^d, Chengfu Yuan ^e, Xiaochuan Sun ^{a,*}, Changdong Wang ^{c,**}

^a Department of Neurosurgery of the First Affiliated Hospital of Chongqing Medical University, Yixueyuan Road #1, Chongqing, 400016, PR China

^b Department of Neurosurgery of the Chongqing Emergency Medical Center, Jiankang Road #1, Chongqing, 400014, PR China

^c Department of Biochemistry and Molecular Biology, Molecular Medicine and Cancer Research Center, Chongqing Medical University, Yixueyuan Road #1, Chongqing, 400016, PR China

^d Department of Microbiology and Molecular Genetics, School of Medicine, University of California, Irvine, Irvine, CA 92697, USA

^e College of Medical Science, China Three Gorges University, Yichang, Hubei, 443002, PR China

Received 10 March 2019; received in revised form 12 May 2019; accepted 20 May 2019

Available online 6 June 2019

KEYWORDS

Traumatic brain injury;
IL-6;
Pioglitazone;
PPAR γ ;
p-NF- κ B

Abstract Traumatic brain injury (TBI) is the major cause of high mortality and disability rates worldwide. Pioglitazone is an activator of peroxisome proliferator-activated receptor- γ (PPAR γ) that can reduce inflammation following TBI. Clinically, neuroinflammation after TBI lacks effective treatment. Although there are many studies on PPAR γ in TBI animals, only few could be converted into clinical, since TBI mechanisms in humans and animals are not completely consistent. The present study, provided a potential theoretical basis and therapeutic target for neuroinflammation treatment after TBI. First, we detected interleukin-6 (IL-6), nitric oxide (NO) and Caspase-3 in TBI clinical specimens, confirming a presence of a high expression of inflammatory factors. Western blot (WB), quantitative real-time PCR (qRT-PCR) and immunohistochemistry (IHC) were used to detect PPAR γ , IL-6, and p-NF- κ B to identify the mechanisms of neuroinflammation. Then, in the rat TBI model, neurobehavioral and cerebral edema levels were investigated after intervention with pioglitazone (PPAR γ activator) or

* Corresponding author.

** Corresponding author.

E-mail addresses: 1422495819@qq.com (Y. Deng), richeljiang@hotmail.com (X. Jiang), XYdeng_cqmu@126.com (X. Deng), hongchen0707@163.com (H. Chen), 494082604@qq.com (J. Xu), 253583549@qq.com (Z. Zhang), 1556985401@qq.com (G. Liu), YongZ4@uci.edu (Z. Yong), Yuancf46@ctgu.edu.cn (C. Yuan), sunxch1445@qq.com (X. Sun), wangchangdong@cqmu.edu.cn (C. Wang).

Peer review under responsibility of Chongqing Medical University.

T0070907 (PPAR γ inhibitor), and PPAR γ , IL-6 and p-NF- κ B were detected again by qRT-PCR, WB and immunofluorescence (IF). The obtained results revealed that: 1) increased expression of IL-6, NO and Caspase-3 in serum and cerebrospinal fluid in patients after TBI, and decreased PPAR γ in brain tissue; 2) pioglitazone could improve neurobehavioral and reduce brain edema in rats after TBI; 3) the protective effect of pioglitazone was achieved by activating PPAR γ and reducing NF- κ B and IL-6. The neuroprotective effect of pioglitazone on TBI was mediated through the PPAR γ /NF- κ B/IL-6 pathway.

Copyright © 2019, Chongqing Medical University. Production and hosting by Elsevier B.V. This is an open access article under the CC BY-NC-ND license (<http://creativecommons.org/licenses/by-nc-nd/4.0/>).

Introduction

Traumatic brain injury (TBI), which has become one of the most common public health problems in both developed and developing countries, is a severe disease burden associated with high mortality and morbidity in all age groups.^{1,2} The mechanisms underlying secondary brain injury are complex, and they involve alterations in cerebral perfusion, activation of inflammatory cytokines and excitotoxicity.³ Neuroinflammation after TBI has a key role in secondary tissue damage, leading to neuronal damage and dysfunction. At present, the surgical intervention is the most common treatment approach, while there are no effective treatments for secondary brain injury after TBI. Therefore, there is an urgent need for new and effective way of relieving neuroinflammation after TBI, thereby improving the prognosis of patients.

PPARs are ligand-activated transcription factors that regulate genes essential for various metabolic processes and cell differentiation, as well as exert anti-inflammatory properties after a brain injury or in patients suffering from neurodegenerative diseases.⁴ Additionally, PPAR agonists exhibit anti-inflammatory and antioxidant effects in several models of CNS disorders, such as ischemic stroke, Alzheimer's, and Parkinson's diseases.^{5–7} Several studies have used both *in vitro* and *in vivo* models to demonstrate PPAR-mediated reduction of the release of pro-inflammatory cytokines and oxidative stress markers.⁸ PPAR γ is a ligand-activated transcription factor from the nuclear receptor family of PPARs. It contains a ligand-binding domain that is hydrophobic and a DNA binding domain of a type II zinc finger structure.⁹

The protective anti-inflammatory effects of PPAR γ are partly mediated through transrepression of the redox-regulated transcription factor nuclear factor kappa B (NF- κ B).^{10,11} As an early transcription factor, activation of NF- κ B does not require regulation of newly translated proteins, making it possible to immediately respond to NF- κ B signaling pathway stimulation of harmful cells.¹² Many molecules involved in the early stages of the immune response and various stages of the inflammatory response are regulated by NF- κ B, including IL-1 β , IL-6, chemokines, adhesion molecules, and colony stimulating factors.^{13,14} Interleukin-6 (IL-6) is involved in a variety of physiological functions including neurodevelopment, hematopoiesis, bone metabolism and immunity.¹⁵

Although there are many studies on PPAR γ and NF- κ B in TBI, there are few transformations or applications in the clinic, which is probably because animal models cannot completely mimic the pathophysiological changes of human TBI. In the current study, we used brain tissue, blood and cerebrospinal fluid of clinical patients combined with animal models of TBI to jointly demonstrate the protective effect of pioglitazone on neuroinflammation, and to provide a feasible theoretical basis and therapeutic target for clinical TBI treatment.

Materials and methods

Reagents and chemicals

Dimethyl sulfoxide (DMSO), pioglitazone, and T0070907, an antagonist of pioglitazone were purchased from Sigma–Aldrich (St. Louis, MO, USA). The primary antibodies for PPAR γ (#24355) and GAPDH (#5174) were obtained from Cell Signaling Technology (CST, Inc, USA). The primary antibodies for p-NF- κ B p65 (Ser536) (ab86299) and IL-6 (ab9324) were acquired from Abcam (Abcam, Cambridge, UK). The secondary antibodies for Western blot and immunohistochemistry were obtained from Santa Cruz Biotechnology (Santa Cruz, CA, USA). Alexa Fluor 555-conjugated anti-rabbit IgG, the secondary antibody for immunofluorescence, was acquired from Invitrogen (Invitrogen, Grand Island, NY). Another the secondary antibody for immunofluorescence DyLight 594 anti-Mouse IgG was purchased from Abbkine (Abbkine, Wuhan).

Human subjects

All clinical case data were obtained from the Department of Neurosurgery of Chongqing Emergency Medical Center. All clinical trials strictly were in strict compliance with the Helsinki Declaration and relevant regulations of Chinese clinical trials, and were approved by the Chongqing Emergency Medical Center Hospital Ethics Committee. The experimental patients or authorized family members informed the experimental content and signed the written informed consent. There was no significant difference in the age and gender between the groups ($P > 0.05$). In addition, serum and cerebrospinal fluid samples were compared between normal group (TBI rehabilitation or cerebral hemorrhage rehabilitation patients: since

hydrocephalus requires lumbar puncture for cerebrospinal fluid examination, some cerebrospinal fluid was taken during lumbar puncture) and TBI group (serum and cerebrospinal fluid samples from TBI surgery patients). Brain tissue samples were also compared between the normal group (the TBI surgery patients resected the contusion edge relative to normal brain tissue) and the TBI group (the TBI surgery patients resected contused brain tissue). Forty-five patients with moderate to severe craniocerebral injury treated with emergency craniotomy and decompression and brain decompression between January 2017 and June 2018 served as the experimental group (all the details on human subjects are specified in the attachment section).

Animals

Sprague–Dawley rats (body weight 180–250 g, age 6–8 weeks) were obtained from Experimental Animal Center of Chongqing Medical University. All the animals were housed in an environment with temperature of 22 ± 1 °C, relative humidity of $50 \pm 1\%$ and a light/dark cycle of 12/12 h, and were fed free diet (sterile pellet feed, standard acidified water). After a few days of feeding, animals were allowed free access to tap water and normal food. All animal studies (including the mice euthanasia procedure) were done in compliance with the regulations and guidelines of Chongqing Medical University institutional animal care and conducted according to the AAALAC and the IACUC guidelines [Experimental Animal Production License: SCXK (Yu) 2018-0003; Laboratory Animal Use License: SYXK (Yu) 2018-0003].

Briefly, a total 134 healthy male rats were randomly divided into 5 following groups according to the random data table method: Sham-operated control group (Sham + DMSO, 24 rats, 0 death), surgery group (TBI + DMSO, 28 rats, 4 deaths), inhibitor group (TBI + T0070907, 29 rats, 5 deaths), treatment group (TBI + pioglitazone, 25 rats, 1 death), anti-treatment group (TBI + T0070907 + pioglitazone, 28 rats, 4 deaths). The dosage details for each experimental rat are shown in the attachment. The time course of all experimental arrangements is shown in the figure (Fig. 1).

Controlled cortical impact model of TBI

According to a previous report, a rat model of controlled cortical impact (CCI) was performed using an electrically controlled pneumatic impact device (TBI 0310, Precision Systems & Instrumentation, Fairfax Station, VA).¹⁶ The device parameters were as follows: impact depth, 5.0 mm from the cortical surface; impact velocity, 6.0 m/sec; residence time, 500 msec. Rats were intraperitoneally anesthetized with 3% pentobarbital (50 mg/kg), and surgery was performed under sterile conditions. A longitudinal incision was made in the midline of the skull, and a 5 mm craniotomy was generated in the left parietal cortex using a portable drill and trephine (craniotomy relative to the center of the anterior iliac crest: 1 mm posterior),¹⁷ removing the bone flap. Rats in the TBI group underwent CCI, while rats in the sham-operated group underwent the

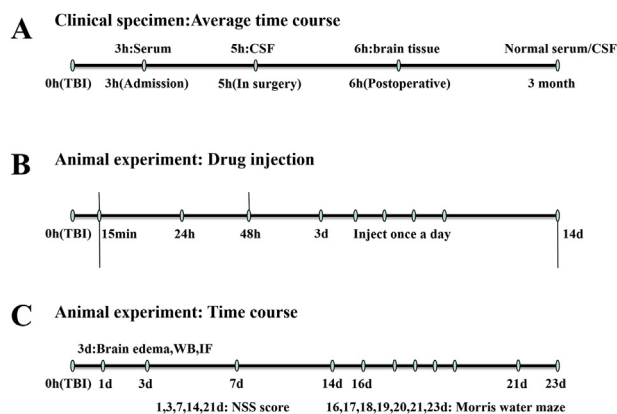


Figure 1 The schematic illustration of the timeline in all experiments.

same surgical procedure, but no trauma occurred in the cerebral cortex. The scalp was closed with cyanoacrylate tissue glue. The body temperature of the rats was monitored and maintained at 37.0 ± 0.5 °C throughout the surgery. According to Serge C's experimental protocol,¹⁸ pioglitazone (1.0 mg/kg), and/or the PPAR γ antagonist T0070907 (1.5 mg/kg) were dissolved in dimethylsulfoxide (DMSO). Sham group and TBI group were given an equal amount of 0.5% DMSO. All injections were administered intraperitoneally. The treatment was initiated 15 min after the CCI operation, and was administered once every 24 h, 48 h. The rats were sacrificed 72 h after the injection, and the samples were taken for subsequent experiments. In particular, according to the timing of the behavioral experiment, the first administration started 15 min after surgery, once a day until 14 days after surgery.¹⁹

Enzyme-linked immunosorbent assay (ELISA)

Evaluation of the concentration of IL-6 (JYM0140140Hu, Wuhan gene col., TD Science and Technology company), and Caspase-3 enzyme (C1115, Beyotime Institute of Biotechnology). The kit was used to detect serum and cerebrospinal fluid samples from patients undergoing TBI surgery.

Measurement of NO

NO was measured using nitrite assay. Nitrite is a relatively stable metabolite of NO. The nitrite concentration was determined with a fluorometric method. Briefly, an aliquot of 100 μ l serum or cerebrospinal fluid samples from patients undergoing TBI surgery was collected at room temperature. After 10–20 min, samples were mixed with 100 μ l of 0.28 M NaOH. The formation of diaminonaphthotriazole, the fluorescent product, was measured using a microplate reader at an excitation wavelength of 355 nm and emission wavelength of 460 nm. A standard curve of NaNO₂ was established for each assay by performing these steps in an identical manner.

Behavioral assays

Neurological severity score (NSS)

The NSS was assessed prior to injury and was repeated three times on days 1, 3, 7, 14 and 21 after CCI as described by Zhang, H.S. et al.²⁰ Using a double-blind approach, the researchers who were blinded to experimental grouping assessed the ability of each rat to perform 10 different tasks. These tasks represented athletic ability, alertness, balance, and general behavior. Failure to complete the task was recorded as one point. The lowest score was 0 points and the maximum score was 10 points.

Morris water maze (MWM)

The MWM test was performed to detect learning latency and spatial memory as previously described by Xiong et al.²¹ The ability to hide the platform in the memory water maze was trained after TBI or from day 16 to day 21 after sham treatment, and the time required for the rats to enter the water to find the platform was recorded, i.e. the incubation period was evaded. Each rat was tested 4 times in different directions each day. The platform was removed on the 23rd day after the injury, and the time delay, the time spent in the correct quadrant, and the time traveled on the platform were recorded by a computer (SLYWMS, Huaibeizhenghua, China).

Brain water content

Seventy-two hours after operation, rats in each group were anesthetized, and after perfusion with 4 °C normal saline, the brain was quickly decapitated, and the brain stem and cerebellum were removed and separated. The brain tissue was weighed and then placed in oven at 110 °C for 24 h (the difference between the two dry weights was less than 0.0002 g). According to the method previously reported in literature,²² the brain tissue water content was calculated as $brain\ water\ content\% = (wet\ weight - dry\ weight) / wet\ weight \times 100\%$.

Quantitative real-time PCR (qRT-PCR)

Total RNA was extracted from samples of human brain tissue using Trizol reagent (Invitrogen, Carlsbad, CA) according to the manufacturer's instructions. cDNA was synthesized from 3 mg of total RNA by the RNA to cDNA EcoDry Premix kit (Clontech, Palo Alto, CA). Quantitative real time PCR (qRT-PCR) experiments were performed with a Bio-RadMJ MiniOption Real Time PCR System in triplicate and the data analysis was carried out by the CFX manager software version 1.5. The PCR data were normalized to GAPDH expression. 10 µl of reaction system, amplification conditions: pre-denaturation at 95 °C for 3 min; 95 °C for 10 s, 56 °C for 30 s, a total of 40 cycles. The sequences of each primer pair were as follows: GAPDH (sense:5'-GAC-CACAGTCCATGCCATCA-3'; antisense:5'-GTCAAAGGTGGAG-GAGTGGG-3'); PPAR γ (sense:5'-GGGGGCATCCCCCTAAACTT-3'; antisense:5'-GCCATGAGGGAGTTGGAAGG-3'); p-NF- κ B (sense:5'-TGGCCCTATGTGGAGATCA -3', antisense:5'-GGG GTTGTGTTGTTGGTCTGGA-3'); IL-6 (sense:5'-CCAGCTAC-GAATCTCCGACC-3', antisense:5'-TATCCTGTCCCTGGAGGT

GG-3'). Calculations were performed according to the 2^{-DeltaDeltaCT} method.

Western blot

The samples of human or rat brain tissues were collected for total protein extraction and the protein concentration measurement kit measures protein concentration. Equal amounts of protein were denatured in SDS and separated on 10% SDS-PAGE gels. Proteins were then transferred to polyvinylidene difluoride (PVDF) membranes. The membranes were blocked with 5% milk, incubated with primary antibody overnight at 4 °C including PPAR γ (diluted 1:1000), p-NF- κ B p65 (Ser536) (diluted 1:2000), IL-6 (diluted 1:2000) and GAPDH (diluted 1:1000), and then incubated with the HRP-labeled secondary antibody (diluted 1:1000) at 37 °C for 2 h, followed by BeyoECL Plus chemiluminescence Method development. The Bio-Rad gel imaging system collects images, and the strips are quantified using the Quantity One software. The GAPDH is set as an internal reference. The experiments were run in triplicate.

Immunohistochemistry

Specimen treatment: Brain tissue samples were taken out from the 4% paraformaldehyde fixative solution, and dehydrated with 80%, 95%, and 100% ethanol solutions in that order. After the xylene was transparent to the brain tissue, the brain tissue was embedded in a wax block for sectioning. The sections were dewaxed and then hydrated with absolute ethanol. Finally, the sections were soaked in 95% ethanol, and rinsed with distilled water three times after each step.

HE staining

The specimen was first stained with hematoxylin for 5 min, then rinsed with distilled water, stained with eosin for 2 min, and then rinsed with distilled water. Dehydration was carried out by using 80%, 95% and 100% ethanol in sequence, and the sections were made transparent with xylene and then fixed with a neutral resin. Finally, they were left to dry and were observed at room temperature.

IHC

After the completion of antigen retrieval, the endogenous enzyme was fired with 0.3% H₂O₂. After blocking 5% BSA at room temperature, the primary antibody PPAR γ (diluted 1:800), p-NF- κ B p65(Ser536) (diluted 1:500) and IL-6 (diluted 1:1000) and the corresponding secondary antibody were sequentially incubated. After 20 min of SABC reagent, staining was performed with a DAB staining kit, and the remaining steps were stained using HE staining.

Immunofluorescence

On day 3 after CCI, rats were deeply anesthetized and perfused with 0.9% saline and 4% paraformaldehyde. The isolated brain was fixed in 4% paraformaldehyde for 24 h, and sucrose (20%, 30%) was dehydrated for 24 h. Then, it was embedded in OCT compound for cryosection, and cut into 10 µm thick coronal sections. Next, Fluorescent

immunolabeling²³ was performed according to standard indirect techniques as previously described. The primary antibodies used included PPAR γ (diluted 1:200), p-NF- κ B p65 (Ser536) (diluted 1:250) and IL-6 (diluted 1:1000). After washing three times in PBS, Alexa Fluor 555-conjugated anti-rabbit IgG or DyLight 594 anti-Mouse IgG was added in PBS with 1% BSA for 1 h. During the final washes, 6-diamidino-2-phenylindole (DAPI) (Sigma) was added and used as a counterstain for nuclei. Fluorescence images were acquired using a Zeiss Axioimager microscope. PPAR γ +/p-NF- κ B +, where IL-6 positive cells were counted in 5 randomly selected regions (200 \times) of each section using Image J software. Immunofluorescence experiments were performed in three brains.

Statistical analysis

All statistical analyses were performed using SPSS software 19.0 (IBM, USA). Values are expressed as mean \pm standard deviation (SD). Based on data from NSS and MWM, two-way analysis of variance (ANOVA) and Student-Newman-Keuls (SNK) tests were used for comparison. Remaining data were evaluated by one-way ANOVA and SNK tests with homogeneity of variance or by Dunnett's post hoc test with square differences. The two groups of clinical specimens were compared using the T-test. $p < 0.05$ was considered to be statistically significant.

Results

High expression of inflammatory factors IL-6, NO and apoptotic factor Caspase-3 in patients with TBI

By detecting clinical specimens, the expressions of IL-6 in serum and cerebrospinal fluid in TBI patients were significantly higher compared to the normal group ($p < 0.05$, Fig. 2A, B). In the same situation, the expressions of NO, caspase-3 in serum and cerebrospinal fluid of patients after TBI were significantly higher than normal group ($p < 0.05$, Fig. 2C–F).

Pioglitazone improved the neurobehavior of rats after TBI to a certain extent, and T0070907 partially inhibited the neuroprotective effect of pioglitazone

To assess the effect of pioglitazone on sensorimotor function, we performed an NSS score. Compared with sham-operated rats, the TBI group showed a significant increase in the NSS score ($p < 0.01$). Compared with the TBI group, the NSS score in the pioglitazone group was significantly reduced ($p < 0.05$). Compared with the pioglitazone group, the T0070907 + pioglitazone group showed a significant increase in the NSS score ($p < 0.05$) (Fig. 3A). These data indicated that the sensorimotor function of rats was

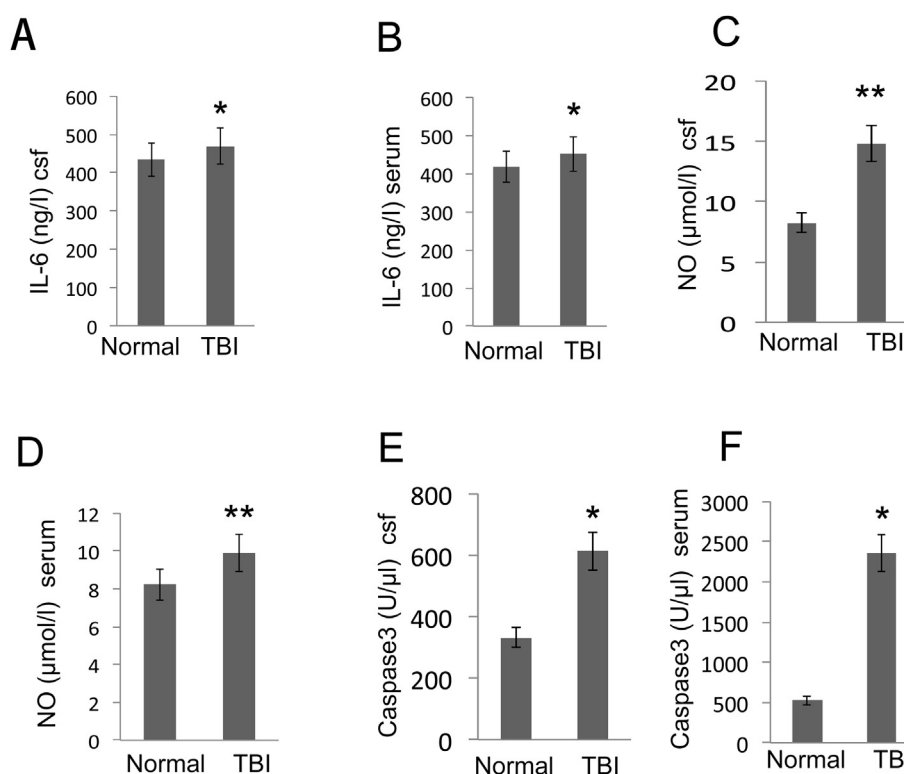


Figure 2 Effect of TBI on IL-6, NO and caspase-3 in CSF and serum. Collection of serum and cerebrospinal fluid in patients during the acute phase of TBI (within 6 h) and during the recovery phase (3 months after surgery). (A–B) IL-6 was evaluated using the IL-6 assay kit from CSF and serum samples. (C–D) The NO concentration was evaluated with an assay kit from CSF and serum samples. (E–F) Effect of TBI on caspase-3 production in CSF and serum. Data are expressed as the mean \pm SD and asterisks indicate statistically significant differences between the TBI ($n = 45$) and Normal groups ($n = 30$). * $p < 0.05$, ** $p < 0.01$ (t-test).

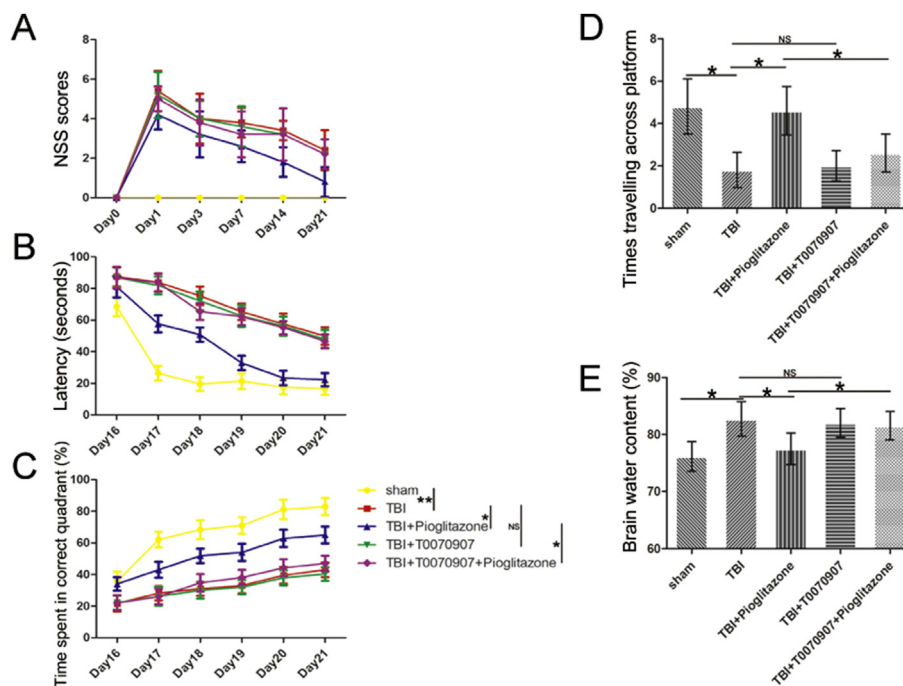


Figure 3 Pioglitazone improved functional outcomes after CCI and brain edema. **(A)** Neurological severity score (NSS) tested prior injury, and on the 1st, 3rd, 7th, 14th and 21st days after CCI [$n = 6/\text{group}$, mean \pm SD and asterisks indicate statistically significant differences between groups (vertical line); $*p < 0.05$, $**p < 0.01$ by two-way ANOVA, NS means no statistically significant differences]. **(B)** Time latency spent in Morris Water Maze (MWM) test from the 16th to the 21st day after CCI [$n = 6/\text{group}$, mean \pm SD and asterisks indicate statistically significant differences between groups (vertical line); $*p < 0.05$, $**p < 0.01$ by two-way ANOVA, NS means no statistically significant differences]. **(C)** Time spent in correct quadrant in spatial learning performance from the 16th to the 21st day after CCI [$n = 6/\text{group}$, mean \pm SD and asterisks indicate statistically significant differences between groups (vertical line); $*p < 0.05$, $**p < 0.01$ by two-way ANOVA, NS means no statistically significant differences]. **(D)** Times traveling across platform on MWM test on the 23rd day after CCI [$n = 6/\text{group}$, mean \pm SD and asterisks indicate statistically significant differences between groups (horizontal line); $*p < 0.05$ by one-way ANOVA, NS means no statistically significant differences]. **(E)** Percentage of brain tissue water content on the 72 h after CCI [$n = 6/\text{group}$, mean \pm SD and asterisks indicate statistically significant differences between groups (horizontal line); $*p < 0.05$ by one-way ANOVA, NS means no statistically significant differences].

impaired after TBI, and pioglitazone could ameliorate this damage, but T0070907 inhibited the therapeutic effect of pioglitazone.

To examine the effect of pioglitazone on learning and memory in rats after TBI, we performed a water maze experiment. Compared with the sham group, the learning and memory ability of the TBI group was significantly decreased ($p < 0.01$), and after the pioglitazone treatment, the learning and memory ability of the rats significantly improved ($p < 0.05$). When T0070907 was added, the effect of pioglitazone was inhibited ($p < 0.05$) (Fig. 3B–D).

Pioglitazone could alleviate brain edema after TBI in rats

Compared with the sham group ($76.17 \pm 4.28\%$), the average brain tissue water content of the TBI group ($86.85 \pm 5.46\%$) was significantly increased ($p < 0.05$). Compared with the TBI group, the pioglitazone group ($78.34 \pm 5.02\%$) had a significant reduction in cerebral edema ($p < 0.05$). When compared with the pioglitazone group, the T0070907 + pioglitazone group ($84.93 \pm 5.53\%$)

was significantly increased ($p < 0.05$) (Fig. 3E). TBI caused the destruction of blood-brain barrier permeability in rats, leading to increased water content in brain tissue; while pioglitazone could maintain blood-brain barrier. T0070907 weakened the protective effect of pioglitazone.

PPAR γ expression was down-regulated in patients with TBI, while pioglitazone increased the expression of PPAR γ after TBI

By detecting clinical specimens, the mRNA and protein level of PPAR γ in TBI patients were significantly reduced compared with the normal group ($p < 0.05$) (Fig. 4A–E). Through immunofluorescence and WB detection in rat brain tissue, PPAR γ was significantly reduced in the TBI group compared with the sham group ($p < 0.05$); PPAR γ was significantly increased in the pioglitazone group after CCI compared with the TBI group ($p < 0.01$). Compared with the pioglitazone group, the T0070907 + pioglitazone group showed a decrease in PPAR γ expression ($p < 0.01$) (Fig. 4G–J). The brain region is shown with an arrow (Fig. 4F).

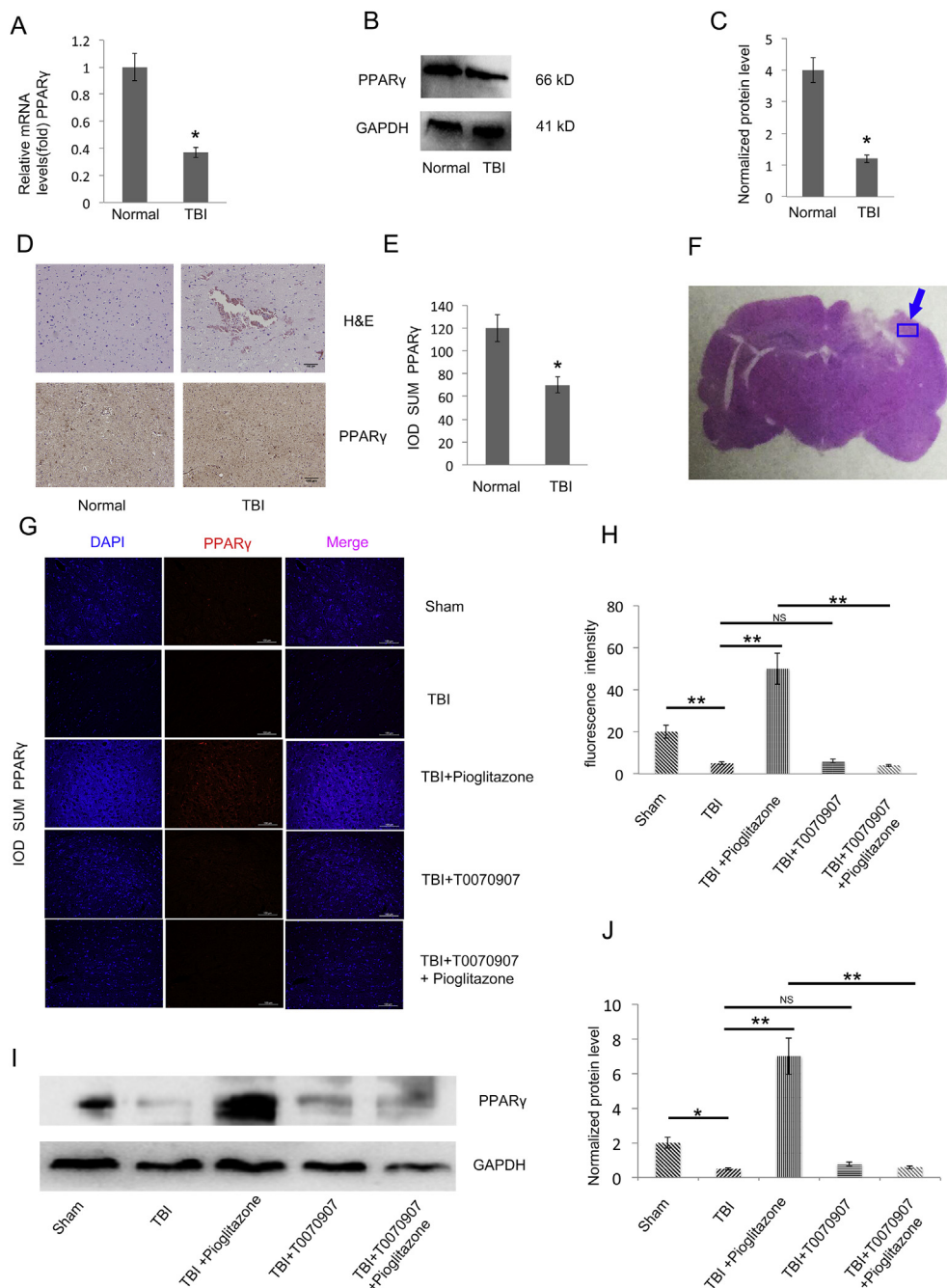


Figure 4 TBI impairs PPAR γ expression. **(A)** qRT-PCR analysis of PPAR γ gene expression in human brain tissue of TBI and normal group (the TBI surgery patients resected the contusion edge relative to normal brain tissue) brain tissues ($n = 25$, triplicates per sample, * $p < 0.05$, t-test). **(B)** Western blot analysis of PPAR γ protein expression in TBI and normal group brain tissues of human ($n = 25$, triplicates per sample). **(C)** Quantification of protein levels from immunoblots as in **B**. The protein levels of PPAR γ were normalized to GAPDH (* $p < 0.05$, t-test). **(D)** Representative clinical human brain tissue of TBI and normal group brain tissue histologic sections of H&E staining (upper right and left panel). Representative histologic sections of PPAR γ staining. The brown color shows positively stained cells by the PPAR γ antibody (lower right and left panel). **(E)** The IOD SUM of positive cells was compared between the TBI and normal groups of human brain tissue ($n = 20$, triplicates per sample, * $p < 0.05$, t-test). **(F)** The rat brain region examined by immunofluorescence **(G)** Representative immunofluorescence images of the surrounding cortex (red: PPAR γ) on the third day after CCI ($n = 6$ /group, scale bar, 100 μ m). **(H)** Quantitative analysis of the fluorescence intensity from immunofluorescence as in **G**. Data were analyzed using an appropriate Student's t-test, one-way ANOVA, or two-way ANOVA followed by post hoc Tukey's analysis. Error bars, SEM.; * $p < 0.05$, ** $p < 0.01$, means statistically significant differences, NS means no statistically significant differences. **(I)** Representative Western blotting images ($n = 6$, triplicates per group). **(J)** Quantification of protein levels from immunoblots as in **I**. The protein levels of PPAR γ were normalized to GAPDH ($n = 6$ /group, mean \pm SD and asterisks indicate statistically significant differences between the two groups shown by horizontal line, * $p < 0.05$, ** $p < 0.01$ by one-way ANOVA, NS means no statistically significant differences).

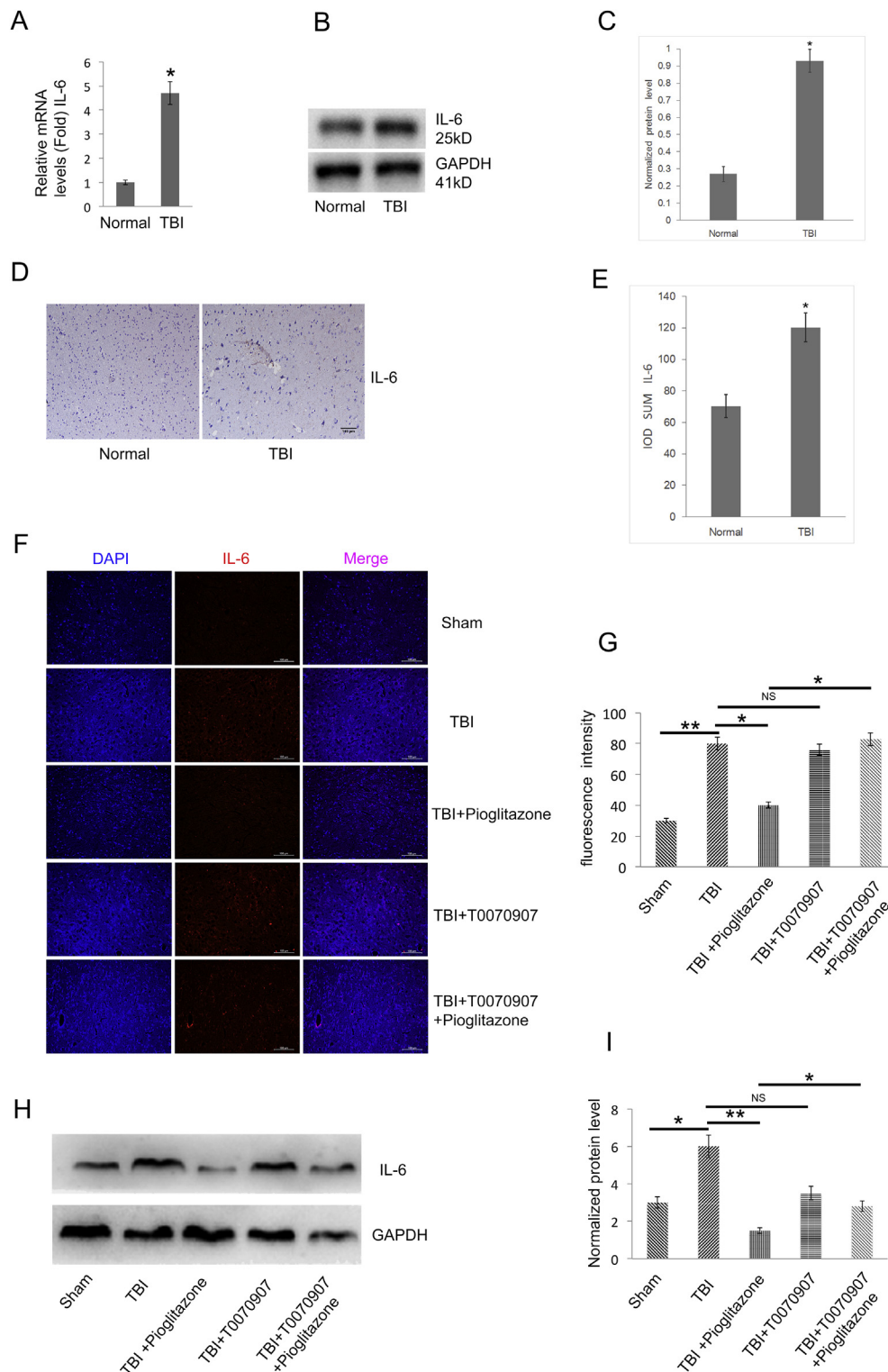


Figure 5 TBI up-regulates the IL-6 level, pioglitazone rescues the effects of TBI, and the effect of pioglitazone was partially reversed by T0070907. (A) qRT-PCR analysis of IL-6 gene expression in human brain tissue of TBI and normal group brain tissues ($n = 25$, triplicates per sample, $*p < 0.05$, t-test). (B) Western blot analysis of IL-6 protein expression in TBI and normal group brain tissues of human ($n = 25$, triplicates per sample). (C) Quantification of protein levels from immunoblots as in B. The protein levels of IL-6 were normalized to GAPDH ($*p < 0.05$, t-test). (D) Representative histologic human clinical TBI and normal group brain tissue sections of IL-6 staining. The brown color shows positively stained cells by the IL-6 antibody. (E) The IOD SUM of positive cells was compared among the TBI and control normal of human brain tissue. ($n = 20$, triplicates per sample, $*p < 0.05$, t-test). (F) Representative immunofluorescence images of the surrounding cortex (red: IL-6) on the third day after CCI ($n = 6$ /group, scale bar, 100 μm). (G) Quantitative analysis of the fluorescence intensity from immunofluorescence as in F. Data were analyzed using an

IL-6 was highly expressed in TBI patients, whereas pioglitazone was observed to reduce IL-6 in the TBI rat model

IL-6 expression was significantly up-regulated in TBI patients compared with the normal group ($p < 0.05$) (Fig. 5A–E). Using IL-6 fluorescent staining and WB, IL-6 was significantly increased in the TBI group compared with the sham group ($p < 0.05$); IL-6 was significantly decreased in the pioglitazone group compared with the TBI group ($p < 0.05$). Compared with the pioglitazone group, T0070907 + pioglitazone group showed an increase in IL-6 expression ($*p < 0.05$) (Fig. 5F–I). The brain region that was studied for the immunofluorescence indicated by the arrow (Fig. 4F).

Overexpression of p-NF- κ B was found in brain tissue of TBI patients, whereas overexpression of p-NF- κ B in rats was effectively reduced by pioglitazone after CCI

qRT-PCR, WB and IHC indicated that p-NF- κ B expression was significantly higher in TBI patients compared to the normal group ($p < 0.05$) (Fig. 6A–E). Based on immunofluorescence and WB detection in rat brain tissue, p-NF- κ B was significantly increased in TBI group compared with sham group ($p < 0.05$). p-NF- κ B was significantly decreased after CCI in pioglitazone group compared with TBI group ($p < 0.05$). Compared with the pioglitazone group, the T0070907 + pioglitazone group showed an increase in p-NF- κ B expression ($p < 0.05$) (Fig. 6F–I). The brain region is shown with an arrow (Fig. 4F).

Discussion

Traumatic brain injury is an important global health problem. TBI can cause death or permanent physical or mental disability. The current view is that pathological changes that occur after TBI in humans and mammals include two stages: primary injury and secondary injury.^{24,25} After irreversible primary injury, TBI leads to a wider range of brain damage through various pathological mechanisms such as inflammatory response, glutamate excitotoxicity, free radical production and lipid peroxidation, ion imbalance, and apoptosis. The secondary injury implies neuronal secondary damage, eventually leading to death.²⁶ Currently, the treatment of choice for TBI patients is usually surgery, while the intervention for various pathophysiological attacks, such as neurological damage caused by neuroinflammation, cerebral edema is still very lacking.

PPAR γ has an important role in many acute and chronic central nervous system diseases such as TBI,²⁷ cerebral ischemia,²⁸ Alzheimer's disease,²⁹ etc. PPAR γ is a ligand-

activated transcription factor belonging to the superfamily of the nuclear hormone receptors. It has been found that PPAR γ receptor activation can promote adipocyte differentiation, enhance and regulate the body's sensitivity to insulin. In addition to regulation of sugar and lipids balance, inhibition of tumor cell growth and participation in cardiovascular protection, it also has an important role in inhibiting the release of inflammatory cells and chemical factors and the formation of inflammation.^{30–33} Pioglitazone is a thiazolidinedione drug and a synthetic agonist of PPAR γ .^{34–36} The anti-inflammatory and neuroprotective effects of pioglitazone on animal models of central nervous system injury and neurodegenerative diseases such as cerebral ischemia, spinal cord injury, experimental autoimmune encephalomyelitis and Parkinson's syndrome have attracted much attention. PPAR γ is activated by binding to pioglitazone, which inhibits cytokines, adhesion molecules and metalloproteinases, as well as inflammatory cells from entering the central region.³¹

The inflammatory response has a key role in secondary brain injury following TBI. The central nervous system inflammatory response is mainly characterized by activation of microglia and astrocytes.^{37,38} Activation of microglia, which produce a variety of cytotoxic substances such as free radicals, superoxide anion, nitric oxide, tumor necrosis factor, interleukin, prostaglandin, etc., lead to neuronal degeneration and necrosis.^{39,40}

In this study, we focused on the first acute brain activity in the TBI and found that the inflammatory factor IL-6 was significantly increased in CSF and serum clinical samples from patients with TBI, indicating that the patient's body was in an inflammatory response. NO also appears to increase in serum and cerebrospinal fluid in patients after TBI, and persistently elevated NO levels can lead to functional impairment of DNA and mitochondria,^{41,42} and can later manifest as neurotoxic effects.^{43,44} Caspase-3 is a key apoptotic protein that is greatly up regulated in CSF and serum of patients with TBI, and that initiates apoptosis of nerve cells surrounding the lesion. All of these results indicate that there are three important biomarkers of IL-6, NO and caspase-3 in acute TBI. Some 2–5 h after the onset of TBI, inflammation, hypoxia and apoptosis are reach severe levels in TBI.

We performed a series of animal behavioral experiments such as NSS scores and Morris water maze in each group of rats, including observation of cerebral edema. We found that nerve function after TBI injury, which aggravated brain edema, could be passed through pioglitazone. In combination with pioglitazone, which is a specific agonist of PPAR γ , we speculated that the above therapeutic effects of pioglitazone occurred due to activation of PPAR γ . On the other hand, during the treatment with pioglitazone, the inhibition of PPAR γ activity by T0070907, the improved neurological function and improved brain edema in rats were

appropriate Student's t-test, one-way ANOVA, or two-way ANOVA followed by post hoc Tukey's analysis. Error bars, SEM.; $*p < 0.05$, $**p < 0.01$, means statistically significant differences, NS means no statistically significant differences. (H) Representative Western blotting images ($n = 6$, triplicates per group). (I) Quantification of protein levels from immunoblots as in H. The protein levels of IL-6 were normalized to GAPDH ($n = 6$ /group, mean \pm SD and asterisks indicate statistically significant differences between the two groups shown by horizontal line, $*p < 0.05$, $**p < 0.01$ by one-way ANOVA, NS means no statistically significant differences).

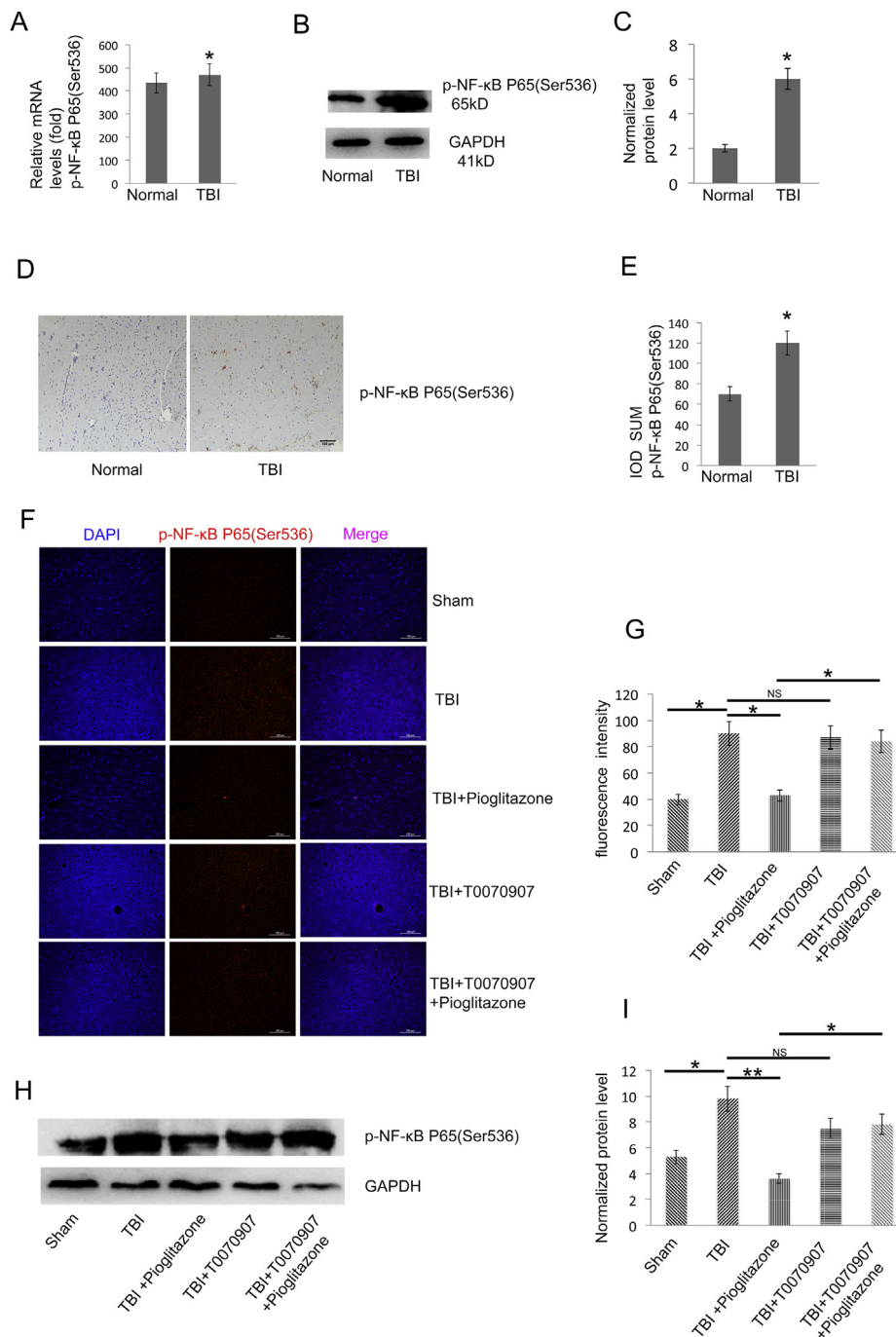


Figure 6 TBI increases the p-NF-κB level and pioglitazone inhibits p-NF-κB protein expression in the TBI rat model. **(A)** qRT-PCR analysis of p-NF-κB gene expression in human brain tissue of TBI and normal group brain tissues ($n = 25$, triplicates per sample, $*p < 0.05$, t-test). **(B)** Western blot analysis of p-NF-κB protein expression in TBI and normal group brain tissues of human ($n = 25$, triplicates per sample). **(C)** Quantification of protein levels from immunoblots as in **B**. The protein levels of p-NF-κB were normalized to GAPDH ($*p < 0.05$, t-test). **(D)** Representative histologic sections of p-NF-κB staining. The brown color shows positively stained cells by the p-NF-κB antibody. **(E)** The IOD SUM of positive cells was compared between the TBI and normal groups of human brain tissue ($n = 20$, triplicates per group, $*p < 0.05$, t-test). **(F)** Representative immunofluorescence images of the surrounding cortex (red: p-NF-κB) on the third day after CCI ($n = 6$ /group, scale bar, 100 μm). **(G)** Quantitative analysis of the fluorescence intensity from immunofluorescence as in **F**. Data were analyzed using an appropriate Student's t-test, one-way ANOVA, or two-way ANOVA followed by post hoc Tukey's analysis. Error bars, SEM.; $*p < 0.05$ means statistically significant differences, NS means no statistically significant differences. **(H)** Representative Western blotting images ($n = 6$, triplicates per group). **(I)** Quantification of protein levels from immunoblots as in **H**. The protein levels of p-NF-κB were normalized to GAPDH ($n = 6$ /group, mean \pm SD and asterisks indicate statistically significant differences between the two groups shown by horizontal line, $*p < 0.05$, $**p < 0.01$ by one-way ANOVA, NS means no statistically significant differences).

partially reversed, which was consistent with our hypothesis.

To further confirm our hypotheses and investigate the potential mechanisms, we obtained brain tissue from TBI patients and slightly higher quantity of normal brain tissue from healthy controls. mRNA, protein and tissue immunohistochemistry showed that the expression intensity of PPAR γ in TBI was comparable to that of the control group; however, the ratio was lower. These clinical data indicated that PPAR γ is affected by TBI and that PPAR γ is functionally reduced. In animal experiments, we also used pioglitazone, which has been shown to reduce cardiovascular risk,⁴⁵ and which rescued TBI's inhibition of PPAR γ . To date, few studies have reported the anti-inflammatory potential of PPAR γ agonists in attenuating TBI-associated inflammatory responses. Although it has been reported that rosiglitazone treatment in primary cultures of rodent astrocytes attenuate LPS-induced secretion of several pro-inflammatory markers (IL-12, TNF α , IL-1 β , IL-6, MCP-1),^{46,47} this effect has not yet been thoroughly examined in astrocytes or microglia in the context of TBI-associated pathologies. Our *in vivo* data demonstrated that glial treatment with pioglitazone reversed TBI-mediated inflammatory responses. Furthermore, we showed that co-administration of a synthetic PPAR γ antagonist, T0070907, which acts as a potent, irreversible, and selective PPAR γ antagonist by modifying a cysteine residue in the ligand-binding site of PPAR γ , abolished the pioglitazone anti-inflammatory effects, thus suggesting that these effects are specifically mediated by PPAR γ .

IL-6 is involved in a variety of physiological functions including neurodevelopment, hematopoiesis, bone metabolism and immunity.¹⁵ In clinical specimens: PCR, western-blot, and tissue immunohistochemistry showed that the expression intensity of IL-6 in TBI was higher than in the control group. In our *in vivo* studies, the pioglitazone inhibited IL-6 protein expression in a rat model of TBI, whereas T0070907 reversed this anti-inflammatory effect of pioglitazone. These data indicated that PPAR γ is a key transcription factor for IL-6 protein expression.

To investigate the mechanisms that are potentially involved in PPAR-mediated anti-inflammatory effects, we examined the effect of pioglitazone treatment on the suppression of the redox-regulated transcriptional factor NF- κ B, up-regulated by TBI. NF- κ B binding sites have been reported in several promoter regions of inflammatory cytokine genes,⁴⁸ and two binding sites have also been identified in the promoter-proximal enhancer region of HIV-1 LTR.⁴⁹ Several mechanisms have been reported for the PPAR γ -mediated inhibition of NF- κ B. These mechanisms include the physical interaction of PPAR γ with NF- κ B; co-activator competition of both transcriptional factors, which regulate protein localization; and prevention of signal-dependent clearance of co-repressor complexes on inflammatory promoters.^{10,50} PPAR γ resulted as an important pathway involved in TBI brain-associated inflammation, which constitutes a potential molecular target for the treatment/prevention of TBI-induced brain inflammation.

In conclusion, this study demonstrates that pioglitazone effectively reduces neuroinflammation after TBI, reduces the extent of cerebral edema, and promotes neurological recovery after TBI. The beneficial effects of pioglitazone

may depend, at least in part, on PPAR γ activation, PPAR γ /NF- κ B/IL-6 signaling pathway that has a key regulatory role in the treatment of TBI with pioglitazone. These data suggest that pioglitazone may be a promising therapeutic approach for the treatment of TBI.

There are some limitations in the present study that need to be pointed out. Since we did not perform any cell experiments *in vitro*, the support for the conclusion is slightly insufficient, which should be addressed by future studies. In addition, pioglitazone cannot be used in TBI patients due to ethical limitations of clinical medications. Nonetheless, our work provides an effective strategy for the prevention and treatment of TBI in the future.

Conflict of interest

The authors declare no conflict of interest.

Acknowledgments

This study was financially supported by the Education Commission of Chongqing in China (Grant No. KJQN201800124 to Y.B. Deng and Grant No. CY170402 to C.D. Wang), the Natural Science Foundation of Chongqing China (Grant No. cstc2016jcyjA0220 to X. Jiang and Grant No. cstc2014jcyjA10024 to C.D. Wang), and Doctoral Program of Higher Education of China (20125503120015 to C.D. Wang).

Appendix A. Supplementary data

Supplementary data related to this article can be found at <https://doi.org/10.1016/j.gendis.2019.05.002>.

References

1. Ghaffarpasand F, Torabi S, Rasti A, et al. Effects of cerebrolysin on functional outcome of patients with traumatic brain injury: a systematic review and meta-analysis. *Neuropsychiatr Dis Treat*. 2018 Dec 27;15:127–135.
2. Arnett E, Weaver AM, Woodyard KC, et al. PPAR γ is critical for *Mycobacterium tuberculosis* induction of Mcl-1 and limitation of human macrophage apoptosis. *PLoS Pathog*. 2018; 14(6):e1007100.
3. Cornelius C, Crupi R, Calabrese V, et al. Traumatic brain injury: oxidative stress and neuroprotection. *Antioxid Redox Signal*. 2013;19(8):836–853.
4. Kurowska P, Chmielinska J, Ptak A, et al. Expression of peroxisome proliferator-activated receptors is regulated by gonadotropins and steroid hormones in *in vitro* porcine ovarian follicles. *J Physiol Pharmacol – Offic J Pol Physiol Soc*. 2017; 68(6):823–832.
5. Barbiero JK, Santiago R, Tonin FS, et al. PPAR-alpha agonist fenofibrate protects against the damaging effects of MPTP in a rat model of Parkinson's disease. *Prog Neuropsychopharmacol Biol Psychiatry*. 2014;53:35–44.
6. Polak PE, Kalinin S, Dello Russo C, et al. Protective effects of a peroxisome proliferator-activated receptor-beta/delta agonist in experimental autoimmune encephalomyelitis. *J Neuroimmunol*. 2005;168(1–2):65–75.
7. Shao ZQ, Liu ZJ. Neuroinflammation and neuronal autophagic death were suppressed via Rosiglitazone treatment: new

- evidence on neuroprotection in a rat model of global cerebral ischemia. *J Neurol Sci.* 2015;349(1–2):65–71.
8. Bernardo A, Minghetti L. Regulation of glial cell functions by PPAR-gamma natural and synthetic agonists. *PPAR Res.* 2008; 2008:864140.
 9. Abbas A, Blandon J, Rude J, et al. PPAR- gamma agonist in treatment of diabetes: cardiovascular safety considerations. *Cardiovasc Hematol Agents Med Chem.* 2012;10(2):124–134.
 10. Ricote M, Glass CK. PPARs and molecular mechanisms of transrepression. *Biochim Biophys Acta.* 2007;1771(8):926–935.
 11. Shang J, Brust R. cooperative cobinding of synthetic and natural ligands to the nuclear receptor PPARgamma. *Elife.* 2018;7.
 12. Liu C, He X, Liu X, et al. *RPS15A Promotes Gastric Cancer Progression via Activation of the Akt/IKK-beta/NF-kappaB Signalling Pathway.* 2019.
 13. Liu Q, Shan P, Li H. Gambogic acid prevents angiotensin ii-induced abdominal aortic aneurysm through inflammatory and oxidative stress dependent targeting the PI3K/Akt/mTOR and NFkappaB signaling pathways. *Mol Med Rep.* 2019 Feb;19(2): 1396–1402.
 14. Shi x, Qiu S, Zhuang W, et al. Follicle-stimulating hormone inhibits cervical cancer via NF-kappaB pathway. *OncoTargets Ther.* 2018;11:8107–8115.
 15. Paige E, Clement M, Lareyre F, et al. Interleukin-6 receptor signalling and abdominal aortic aneurysm growth rates. *Circ Genom Precis Med.* 2019 Feb;12(2), e002413.
 16. Wang W, Li H, Yu J, et al. Protective effects of Chinese herbal medicine *Rhizoma drynariae* in rats after traumatic brain injury and identification of active compound. *Mol Neurobiol.* 2016;53(7):4809–4820.
 17. Xing Z, Xia Z, Peng W, et al. Xuefu Zhuyu decoction, a traditional Chinese medicine, provides neuroprotection in a rat model of traumatic brain injury via an anti-inflammatory pathway. *Sci Rep.* 2016;6:20040.
 18. Thal SC, Heinemann M, Luh C, et al. Pioglitazone reduces secondary brain damage after experimental brain trauma by PPAR-gamma-independent mechanisms. *J Neurotrauma.* 2011; 28(6):983–993.
 19. He J, Liu H, Zhong J, et al. Bexarotene protects against neurotoxicity partially through a PPARgamma-dependent mechanism in mice following traumatic brain injury. *Neurobiol Dis.* 2018;117:114–124.
 20. Zhang HS, Li H, Zhang DD, et al. Inhibition of myeloid differentiation factor 88(MyD88) by ST2825 provides neuroprotection after experimental traumatic brain injury in mice. *Brain Res.* 2016;1643:130–139.
 21. Xiong Y, mahmood A, Qu C, et al. Erythropoietin improves histological and functional outcomes after traumatic brain injury in mice in the absence of the neural erythropoietin receptor. *J Neurotrauma.* 2010;27(1):205–215.
 22. Sakamoto J, Miura T, Shimamoto K, et al. Predominant expression of Sir2alpha, an NAD-dependent histone deacetylase, in the embryonic mouse heart and brain. *FEBS Lett.* 2004; 556(1–3):281–286.
 23. Han L, Cai W, Mao L, et al. Rosiglitazone promotes white matter integrity and long-term functional recovery after focal cerebral ischemia. *Stroke.* 2015 Sep;46(9):2628–2636.
 24. Dai X, Yi M, Wang D, et al. Changqin NO. 1 inhibits neuronal apoptosis via suppressing GAS5 expression in traumatic brain injury mice model. *Biol Chem.* 2019 May 27;400(6):753–763.
 25. Fama F, Vita R, Sindoni A, et al. High frequency of empty sella, with gender differences, in the early neuroradiology evaluation of patients with traumatic brain injury. A prospective study. *J Clin Transl Endocrinol.* 2018 Dec 31;15:54–61.
 26. Sun M, Brady RD, Van Der Poel C, et al. A concomitant muscle injury does not Worsen traumatic brain injury outcomes in mice. *Front Neurol.* 2018 Dec 11;9.
 27. Mishra AK, Klein C, Gurcha SS, et al. Structural characterization and functional properties of a novel lipomannan variant isolated from a *Corynebacterium glutamicum pimB'* mutant. *Antonie van Leeuwenhoek.* 2008;94(2):277–287.
 28. Li Q, Tian Z, Wang M, et al. Luteoloside attenuates neuroinflammation in focal cerebral ischemia in rats via regulation of the PPARgamma/Nrf2/NF-kappaB signaling pathway. *Int Immunopharmacol.* 2019;66:309–316.
 29. Govindarajulu M, Pinky PD. Signaling mechanisms of selective PPARgamma modulators in Alzheimer's disease. *PPAR Res.* 2018;2018, 2010675.
 30. Clark RB. The role of PPARs in inflammation and immunity. *J Leukoc Biol.* 2002;71(3):388–400.
 31. Nencioni A, Wesselborg S, Brossart P. Role of peroxisome proliferator-activated receptor gamma and its ligands in the control of immune responses. *Crit Rev Immunol.* 2003;23(1–2): 1–13.
 32. Ota N, Soga S, Haramizu S, et al. Tea catechins prevent contractile dysfunction in unloaded murine soleus muscle: a pilot study. *Nutrition (Burbank, Los Angeles County, Calif).* 2011; 27(9):955–959.
 33. Pierzchalski P, Krawiec A, Gawelko J, et al. Molecular mechanism of protection against chemically and gamma-radiation induced apoptosis in human colon cancer cells. *J Physiol Pharmacol – Offic J Pol Physiol Soc.* 2008;59(Suppl 2): 191–202.
 34. Desvergne B, Wahli W. Peroxisome proliferator-activated receptors: nuclear control of metabolism. *Endocr Rev.* 1999; 20(5):649–688.
 35. Culman J, Zhao Y, Gohlke P, et al. PPAR-gamma: therapeutic target for ischemic stroke. *Trends Pharmacol Sci.* 2007;28(5): 244–249.
 36. Ouk T, Potey C, Gautier S, et al. PPARs: a potential target for a disease-modifying strategy in stroke. *Curr Drug Targets.* 2013; 14(7):752–767.
 37. Finsen B, Owens T. Innate immune responses in central nervous system inflammation. *Immunology.* 2011;585(23):3806–3812.
 38. Griffiths MR, Botto M, Morgan BP, et al. CD93 regulates central nervous system inflammation in two mouse models of autoimmune encephalomyelitis. *Immunology.* 2018;155(3): 346–355.
 39. Dey A, Allen JN, Fraser JW, et al. Neuroprotective role of the Ron receptor tyrosine kinase underlying central nervous system inflammation in health and disease. *Front Immunol.* 2018;9: 513.
 40. Voet S, Prinz M, Van Loo G. Microglia in central nervous system inflammation and multiple sclerosis pathology. *Trends Mol Med.* 2019 Feb;25(2):112–123.
 41. Gupta S, Goswami P, Biswas J, et al. 6-Hydroxydopamine and lipopolysaccharides induced DNA damage in astrocytes: involvement of nitric oxide and mitochondria. *Mutat Res Genet Toxicol Environ Mutagen.* 2015;778:22–36.
 42. Mikhed Y, Daiber A, Steven S. Mitochondrial oxidative stress, mitochondrial DNA damage and their role in age-Related vascular dysfunction. *Int J Mol Sci.* 2015;16(7): 15918–15953.
 43. Krishna G, Muralidhara. Oral supplements of combined fructo- and xylo-oligosaccharides during perinatal period significantly offsets acrylamide-induced oxidative impairments and neurotoxicity in rats. *J Physiol Pharmacol – Offic J Pol Physiol Soc.* 2018;69(5).
 44. Zhang Y, Zhu Z, Liang HY, et al. nNOS-CAPON interaction mediates amyloid-beta-induced neurotoxicity, especially in the early stages. *Aging Cell.* 2018;17(3):e12754.
 45. Dormandy JA, Charbonnel B, Eckland DJ, et al. Secondary prevention of macrovascular events in patients with type 2 diabetes in the PROactive Study (PROspective pioglitAZone Clinical Trial in macroVascular Events): a randomised

- controlled trial. *Lancet (London, England)*. 2005;366(9493):1279–1289.
46. Xu J, Drew PD. Peroxisome proliferator-activated receptor-gamma agonists suppress the production of IL-12 family cytokines by activated glia. *J Immunol*. 2007;178(3):1904–1913.
 47. Storer PD, Xu J, Chavis J, et al. Peroxisome proliferator-activated receptor-gamma agonists inhibit the activation of microglia and astrocytes: implications for multiple sclerosis. *J Neuroimmunol*. 2005;161(1–2):113–122.
 48. Hoesel B, Schmid JA. The complexity of NF-kappaB signaling in inflammation and cancer. *Mol Cancer*. 2013;12:86.
 49. Hiscott J, Kwon H, Genin P. Hostile takeovers: viral appropriation of the NF-kappaB pathway. *J Clin Invest*. 2001;107(2):143–151.
 50. Sauer S. Ligands for the nuclear peroxisome proliferator-activated receptor gamma. *Trends Pharmacol Sci*. 2015;36(10):688–704.